CMS RESULTS ON SMALL-x QCD*

Maciej Misiura

on behalf of the CMS Collaboration

University of Warsaw, Faculty of Physics
Hoża 69, 00-681 Warszawa, Poland

(Received April 16, 2013)

Three CMS measurements sensitive to small-x QCD and multi-parton interactions are discussed: forward energy flow, inclusive cross-sections for forward jets production and inclusive to exclusive dijets production cross-sections ratios. Results are compared to predictions of various Monte Carlo models.

DOI:10.5506/APhysPolB.44.1545
PACS numbers: 12.38.Aw, 12.38.Bx

1. Introduction

Due to large calorimetric coverage, data collected by the Compact Muon Solenoid (CMS) detector at the CERN Large Hadron Collider (LHC) provides valuable testing ground for the QCD in the low-x region. The variable x denotes here the fraction of the proton longitudinal momentum carried by an interacting parton. In this paper, three measurements sensitive to low-x processes are described: (1) measurement of the energy flow (*i.e.* average energy per event), (2) measurement of inclusive cross-sections for forward jets production and (3) measurement of inclusive to exclusive dijets production cross-sections ratios. Measurement (1) is sensitive to multi-parton interactions (MPI) and opens a new region of the phase space, where MPI models can be tuned. One of the aims of (2) and (3) is the search for signs of BFKL evolution in the data. In the low-x region, the standard approach to QCD perturbative calculations, where powers of $\log(Q^2)$ are summed, (DGLAP) may not be sufficient. The alternative is BFKL evolution, where powers of $\log(1/x)$ are summed.

* Presented at the Cracow Epiphany Conference on the Physics After the First Phase of the LHC, Kraków, Poland, January 7–9, 2013.

2. Experimental setup

A complete description of the CMS detector can be found in [1]. In this section, a brief description of selected detector subsystems especially important for the presented analyses is given.

To measure momenta of charged particles, CMS uses a superconducting solenoid that provides 3.8 T magnetic field parallel to the beam axis. Tracks of charged particles are measured by silicon pixel detectors and strip trackers for pseudorapidity $|\eta| < 2.5$. Electromagnetic calorimeter (ECAL) and hadronic calorimeter (HCAL) extend to $|\eta| < 3$. ECAL is lead tungstate crystal calorimeter with cells grouped in towers of size $\Delta\eta \times \Delta\phi = 0.0174 \times 0.0174$ in the central part of the detector ($|\eta| < 1.5$) and 0.05×0.05 in $1.5 < |\eta| < 3.0$ region. The HCAL is a sampling calorimeter made of alternating layers of the absorber and the scintillator. The segmentation in the central part of HCAL is 0.087×0.087 and 0.17×0.17 in $1.6 < |\eta| < 3$. The Hadronic Forward (HF) calorimeter is the calorimeter covering the most forward pseudorapidity region from $|\eta| = 3$ to $|\eta| = 5.2$. The HF detector is located 11.2 m from the nominal interaction point and consists of steel absorbers containing embedded quartz fibres. The granularity of HF is 0.175×0.175 up to $|\eta| < 4.7$ and 0.175×0.35 at larger pseudorapidities.

3. Energy flow at large pseudorapidities

In the analysis described in [2], the QCD is tested by a measurement of the energy flow. Energy flow is defined as an average energy deposited in the detector per event. Results for the data are compared to predictions of different Monte Carlo models. The measurement is limited to the forward region of the detector and only energy deposits in the HF detector are taken to the energy flow calculation ($3 < |\eta| < 4.9$). The energy flow is measured in bins of the pseudorapidity. The measurement was performed for two collision energies: $\sqrt{s} = 7$ TeV and $\sqrt{s} = 900$ GeV. Only a small fraction of data collected at the beginning of 2010 was included in the analysis: 239 μb^{-1} for a 0.9 TeV and 206 μb^{-1} for 7 TeV, to avoid high pile-up. The probability of having an additional proton–proton interaction in a given bunch crossing was estimated to be 1%.

For each energy, two subsamples were considered: the minimum-bias and the hard scale sample. For the minimum-bias sample, a special minimum-bias trigger was used with an additional requirement of a reconstructed vertex in the event. In the hard scale sample, the presence of a dijet system consisting of two jets in the central region of the detector ($|\eta| < 2.5$) was required. The cut on jets transverse momentum was $p_{\text{T}} > 8$ GeV for $\sqrt{s} = 900$ GeV and $p_{\text{T}} > 20$ GeV for $\sqrt{s} = 7$ TeV. The separation between jets in the transverse plane was limited to $|\Delta\phi - \pi| < 1$, where $\Delta\phi$ is a difference of angular angles of jets, to provide good dijet p_{T} balance.

Results for the data are compared to different Monte Carlo generators that have different physical models implemented. Predictions of PYTHIA6 with Tevatron tunes: DW, Pro-Q20, Pro-pT0 and LHC tunes: Z2, P11, AMBT1 are shown. Additionally predictions of PYTHIA8 (no tuning), Herwig++ (different hadronization model than in PYTHIA), CASCADE (CCFM evolution) and DIPSY (based on BFKL) are presented. Results for the data were corrected to the stable particle level using bin-by-bin correction factors.

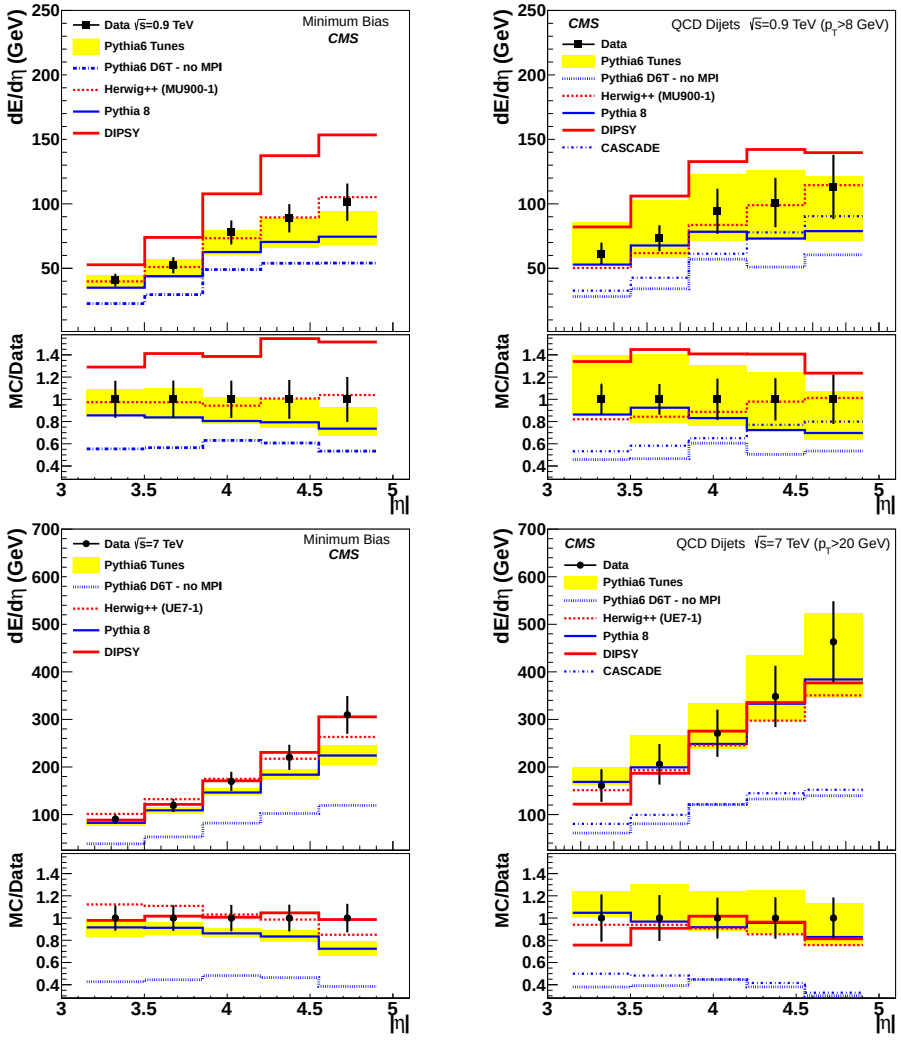

Fig. 1. Results of the forward energy flow measurement for $\sqrt{s} = 900$ GeV (top) and $\sqrt{s} = 7$ TeV (bottom) and for minimum bias (left) and dijet (right) samples.

Results of the analysis are presented in Fig. 1. Error bars represent the systematic uncertainty, the statistical uncertainty is negligible. The energy flow for all samples grows with η and is larger for the hard scale sample than for the minimum bias sample. In Fig. 1, predictions of different Monte Carlo models are also shown. The grey (yellow) band is composed from predictions of different PYTHIA6 tunes. For the minimum bias sample, PYTHIA6 and PYTHIA8 results are consistent with the data within statistical uncertainties. PYTHIA6 D6T without MPI and CASCADE do not describe the data. The inclusion of MPI in modelling is necessary. DIPSY describes data only for 7 TeV sample. Herwig++ provides good description for both energies, while PYTHIA8 describes data only for 7 TeV. For the hard scale sample, the description of data by models is more accurate.

4. Forward and forward–central jets

One of the tools that may be useful in exploration of low-x physics are forward jets, *i.e.* jets emitted at small polar angles with pseudorapidity $|\eta| > 3$. Such jets usually come from asymmetric collisions: x of one patron taking part in the hard interaction is much smaller than x of the other parton. The aim of the analysis presented in [3] was the measurement of the differential inclusive cross-sections for *(i)* a production of the forward jet ($3.2 < |\eta| < 4.7$) and *(ii)* a production of the forward jet associated with a jet emitted in the central part of the detector ($|\eta| < 2.8$). Cross-sections were measured as a function of the transverse momentum p_{T} of forward jet in cases *(i)* and *(ii)* and in the case *(ii)*, additionally, as a function of the central jet p_{T}. Jets

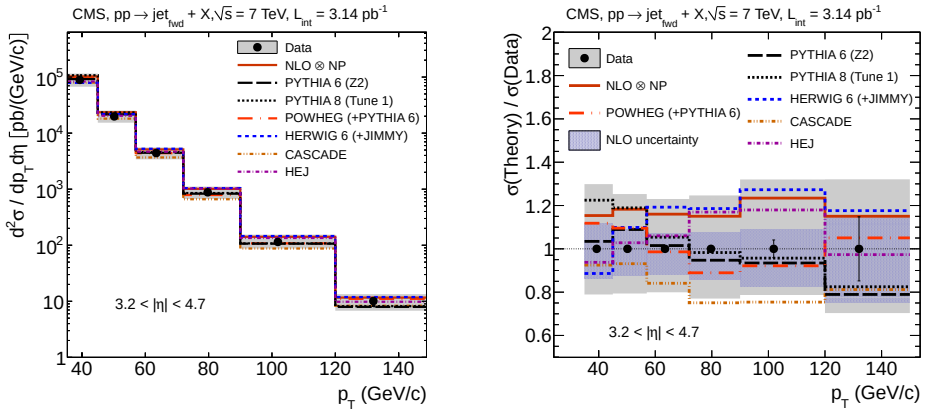

Fig. 2. Results of the measurement of inclusive cross-section for the forward jet production (left) compared to the predictions of different Monte Carlo generators and NLO calculations. The ratio of the theoretical predictions to the data is presented in the right plot.

were reconstructed with the anti-k_{T} algorithm with the cone radius $R = 0.5$ and only jets with $p_{\mathrm{T}} > 35$ GeV were taken into the analysis. Data were collected in 2010 with dedicated triggers selecting events with jet and dijets presence. The sample corresponding to integrated luminosity of 3.14 pb^{-1} was analysed. The presence of at least one reconstructed primary vertex in the event was required. An average number of proton–proton interactions in one bunch crossing in the analysed data sample was estimated to be 2.2. Results for the data were corrected for the detector effects, such as the finite measurement resolution, and unfolded with the bin-by-bin method to the stable particle level. The uncertainty from the model dependence of that correction (±10%) was included in the systematic uncertainty. Other sources of the uncertainty were: the uncertainty of the luminosity determination (±4%) and the uncertainty of the Jet Energy Scale determination (from 3% to 6%, depending on η and p_{T}).

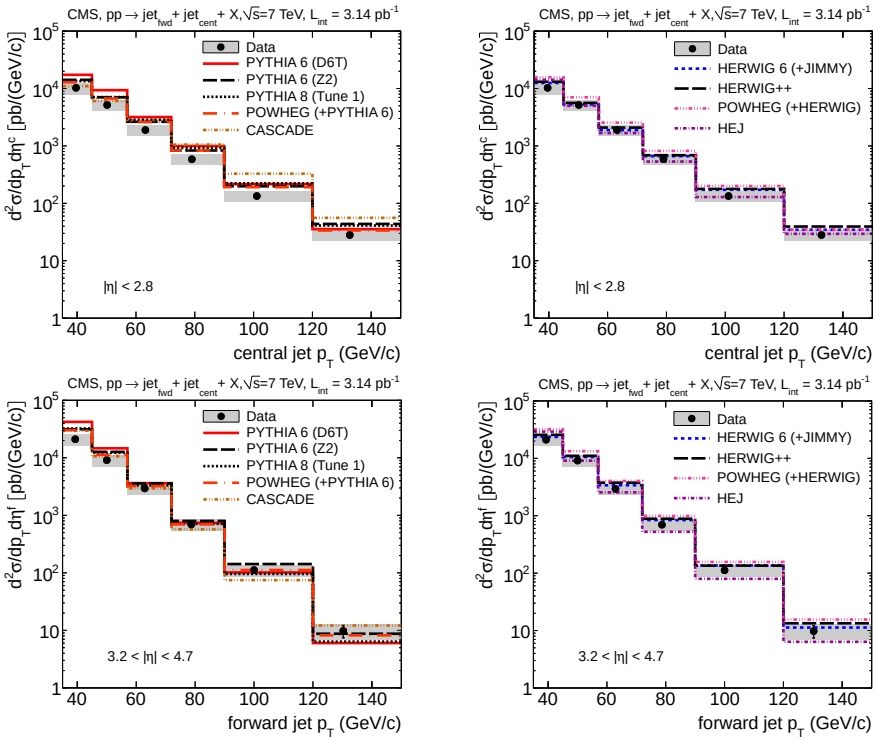

Fig. 3. Results of the measurement of inclusive cross-section for the production of a forward jet associated with a central jet as a function of the central jet p_{T} (top plots) or the forward jet p_{T} (bottom plots). Results for the data are compared to PYTHIA6, PYTHIA8, POWHEG (+PYTHIA), CASCADE predictions (left) and to HERWIG6, Herwig++, POWHEG (+Herwig), HEJ predictions (right).

Results for the data are compared to predictions of various Monte Carlo generators. The general purpose generators basing on the DGLAP approach are PYTHIA6 (tunes D6T, Z2), PYTHIA8 with Tune 1, HERWIG6 with JIMMY package for underlying event modelling and Herwig++. Data is also compared to NLO calculations (POWHEG and NLOJET++ as implemented in FastNLO package) corrected for the non-perturbative effects as well as to the prediction of the CASCADE Monte Carlo generator.

The inclusive forward jet spectrum corrected for the detector effects is shown in Fig. 2. Results for data are compared to predictions of different models. Within theoretical and experimental uncertainties, the measured values are in agreement with predictions of theoretical models.

Results for forward–central jet spectrum are presented in Fig. 3. Results are presented as a function of p_{T} of the central and the forward jet in the dijet. Ratios of data to theory for these distributions are presented in Fig. 4. The best predictions are provided by HERWIG6 and Herwig++. Other considered models tend to predict larger values of cross-sections than observed in the data. The description of the central jets spectrum is worse than the forward jets spectrum.

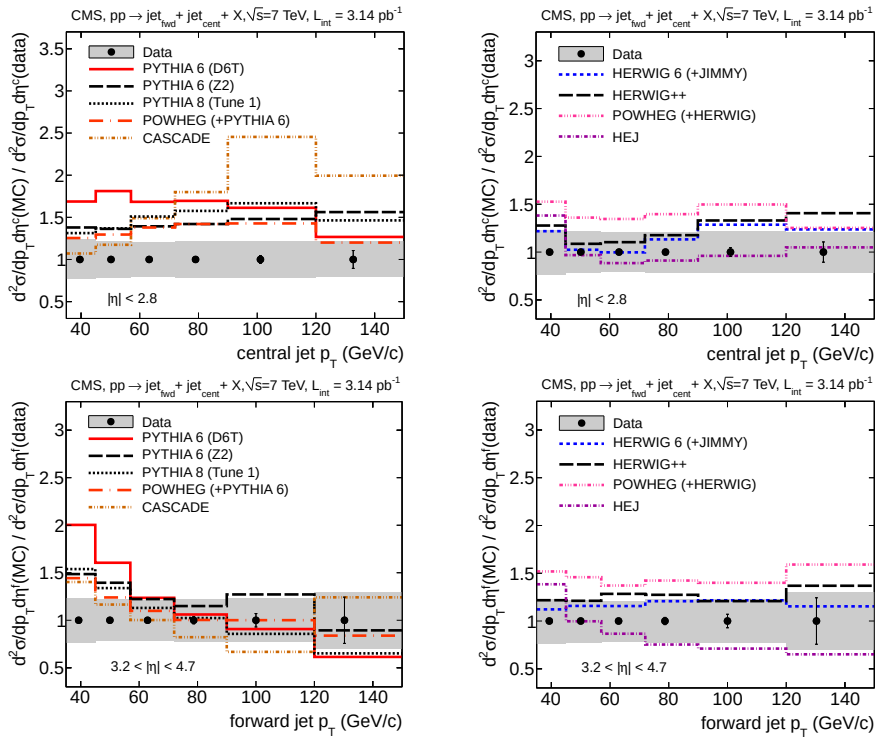

Fig. 4. Ratios of theory predictions to data for distributions presented in Fig. 3.

5. Ratios of dijet production cross-sections

In this study, ratios of cross-sections for dijets production are determined. For the analysis, only events with at least one pair of jets passing cuts $p_{\mathrm{T}} > 35$ GeV and $|\eta| < 4.7$ are taken. The inclusive cross-section σ_{incl} is obtained by taking all pairwise combinations of jets in the event. The exclusive cross-section σ_{excl} is then measured from a subsample of events containing only one pair of jets. Additionally, Mueller–Navelet sample is defined, taking from all combinations of jet pairs the one with the largest $\Delta\eta$ separation. The corresponding cross-section is denoted as σ_{MN}. One of the variables that could be sensitive to BFKL effects are ratios of cross-sections: $R^{\mathrm{incl}} = \sigma_{\mathrm{incl}}/\sigma_{\mathrm{excl}}$ and $R^{\mathrm{MN}} = \sigma_{\mathrm{MN}}/\sigma_{\mathrm{excl}}$. Ratios are measured as a function of $\Delta\eta$, *i.e.* separation between the jets. BFKL effects should be stronger at large separation in pseudorapidity, as the phase space for additional radiation is larger. The experimental advantage of measuring the ratios is the cancellation of these systematical effects that are the same in numerator and denominator. Additionally, presence of exactly one primary vertex in the event is required. That cut reduces significantly the influence of pile-up on the measured values. The data were collected in 2010 and samples selected with two jet triggers were mixed to obtain high efficiency for events with large $\Delta\eta$ that are rare. Results for the data are corrected to the stable particle level.

Results of the measurement are presented in Fig. 5 and compared to the predictions of various Monte Carlo generators. PYTHIA6 tune Z2 and PYTHIA8 tune 4C agree with the measurement within systematical uncertainty presented as the grey (yellow) band. Predictions of Herwig++ and HEJ (+Ariadne) are larger than results for the data. Discrepancies are getting larger as the separation in pseudorapidity is being increased. CASCADE predicts ratios much larger than observed in the data.

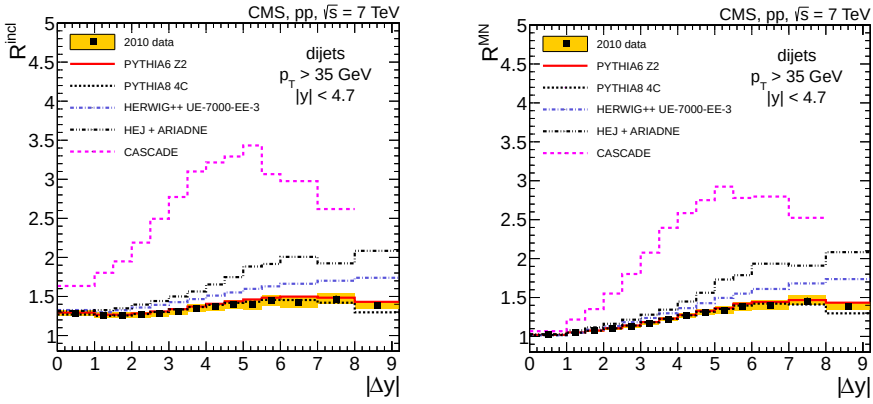

Fig. 5. Results for the measurements of R^{incl} and R^{MN} as a function of $\Delta\eta$.

6. Summary

Three measurements in the low-x region of the phase space have been presented. The energy flow measurement showed that proper simulation of MPI is important for a good description of data by Monte Carlo generators. In the presented jet measurements, there is no clear evidence for the presence of BFKL effects in the data. There are some discrepancies between predictions and the data that should be further studied.

REFERENCES

[1] CMS Collaboration, *JINST* **03**, S08004 (2008).

[2] CMS Collaboration, *J. High Energy Phys.* **1111**, 148 (2011) [arXiv:1110.0211 [hep-ex]].

[3] CMS Collaboration, *J. High Energy Phys.* **1206**, 036 (2012) [arXiv:1202.0704 [hep-ex]].

[4] CMS Collaboration, *Eur. Phys. J.* **C72**, 2216 (2012) [arXiv:1204.0696 [hep-ex]].